■ 原著

訓練機器を用いた大腿四頭筋セッティングにおける筋活動性に対する検討

穐丸　舞[1)]　縄田　厚[1)]　岩嵜徹治[1)]　古賀良生[2)]
大森　豪[4)]　遠藤和男[5)]　渡辺博史[3)]

アルケア株式会社医工学研究所[1)]，新潟こばり病院整形外科[2)]，同リハビリテーション部[3)]，
新潟大学超域研究機構[4)]，新潟医療福祉大学健康科学部[5)]

要旨　本研究は，下肢筋力訓練方法の効果の明確化を目的とし，健常者を対象に機器を用いた大腿四頭筋セッティング（以下，Q-セッティング）の効果および他の訓練との違いを筋電図にて分析した．その結果Q-セッティングでの大腿四頭筋の筋活動は，他の訓練と同等以上であり，固定なしQ-セッティングでは内側ハムストリングの筋活動が有意に大きかった．Q-セッティングの方法を変えることで目的に合った訓練ができると示唆された．

Abstract　In this study, we have investigated the effect of instrument for quadriceps setting (with or without fixation of ankle and pelvis) and comparison with instrument for quadriceps setting and other training methods (straight leg raising and knee extension) by using electromyogram.

As a result, the lower limb muscle activity by quadriceps setting method was equivalent performance compared with other training. And medial hamstring activity by quadriceps setting method without fixation was higher performance than other training. We concluded that it is useful training method to enhance the muscle activity with using instrument for quadriceps setting.

Key words：大腿四頭筋セッティング（quadriceps setting），筋電図（electromyogram），機器を用いた筋力トレーニング（muscle training using the instrument）

はじめに

大腿四頭筋に対する等尺性運動は安全性に優れた方法であり[8)]，変形性膝関節症の保存的治療において多く用いられている[1,3)]．しかし，臨床の現場における実際の筋力訓練は一律に行われることが多く，個人差を考慮し定量化された方法での訓練は一般に行われていない．

われわれは，筋力の評価および筋力強化訓練の効率を向上させるために等尺性運動であるQ-セッティングに対する簡易筋力測定・訓練機を開発し，その有用性について報告してきた[5,7)]．大腿四頭筋訓練にはさまざまな

Electromyographic analysis of quadriceps setting using the exercise instrument
Mai AKIMARU, Atsushi NAWATA, Tetsuji IWASAKI, Yoshio KOGA, MD, Go OMORI, MD, Kazuo ENDO, MD and Hiroshi WATANABE, RPT

連絡先：〒131-0046 東京都墨田区京島 1-21-10　アルケア株式会社医工学研究所　穐丸　舞　電話 03-3611-1101

方法があり，より効率的な筋力向上を考えた場合，異なる訓練法がどのように下肢筋力に効果をもたらしているのかを明確にすることは必要である．本研究では，われわれが開発した筋力訓練機器を用いたQ-セッティングの効果を筋活動の点から他の筋力訓練方法と比較検討した．

対象および方法

1．対象

対象は，あらかじめ本研究の主旨および内容を説明し，研究協力に同意の得られた健常な成人男女10名（男性7名，女性3名）とし，平均年齢は37.0±11.8歳であった．

2．測定内容

測定を行った訓練は，Q-セッティング（固定あり，固定なし）とRCT（randomized controlled trial）によって有効性が確認されているstraight leg raising（以下，SLR）[3]や膝伸展運動の4種類とした．まず，いずれの訓練においても後述する方法で最大筋力発揮時の筋活動を測定した．次に，Q-セッティング（固定あり，固定なし）およびSLRについては，機器による負荷力設定時の比較のために，最大筋力に対する60%筋力発揮時の筋活動を計測した．膝伸展運動は各訓練における筋活動量を比較するための基準値として測定し，本試験における分析・評価を実施した．また，すべての測定は右下肢で行った．

3．使用機器

筋活動測定には表面筋電図（以下，EMG：NECメディカルシステムズ社製のサイナアクトMT11）を使用し，電極はAmbu製の使い捨て型表面電極（Blue Sensor）を使用した．

Q-セッティングにおける最大筋力の測定および60%筋力測定（設定）には，われわれが開発した下肢筋力測定訓練機（QTM-05F）（以下，測定器）[5]を用いた（図1）．また，SLRにおける最大筋力の測定，および60%筋力測定には島津製作所製のオートグラフAG-I 20 kNを使用した．

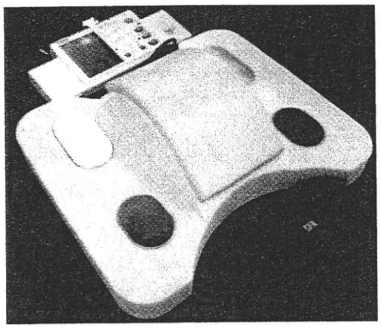

図1 下肢筋力測定訓練機
機器は，本体計測部と表示・操作部にて構成され，表示・操作部の指示にて操作できる構造となっている．

4．筋活動の測定評価方法

EMGのサンプリング周波数は1,000 Hzとし，アースは上前腸骨棘とした．それぞれの部位に対し皮膚の電気抵抗を下げるために，あらかじめ抵抗が10 Ω以下になるように皮膚抵抗を落とした．電極は中心距離30 mmで各筋の筋線維の走行に平行に貼付した．被験筋は前脛骨筋（TA），腓腹筋（GC），外側広筋（VL），大腿直筋（RF），内側広筋（VM），外側ハムストリング（HL），内側ハムストリング（HM）の7筋とした．得られたEMG信号はA/D変換後CSV形式で保存し，全波整流化後，筋放電量が一定になった時点（波形が安定した時点）から3秒間の積分値を採用した．正規化するため膝伸展運動の積分値を100%とし，各データは膝伸展運動の積分値で除して%IEMGとした．

5．筋力測定方法

各測定肢位は，以下のように定義した．

固定ありQ-セッティングの測定姿勢は，

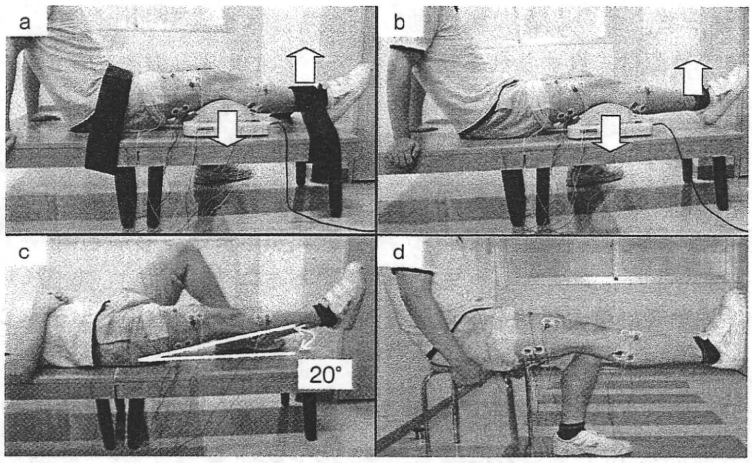

図2 訓練別筋力測定肢位

a：固定ありQ-セッティング．骨盤と下腿遠位部を非伸縮バンドで固定して矢印の方向に力を加え，膝伸展運動をさせた際の膝窩部に発生する力を測定した．

b：固定なしQ-セッティング．固定ありQ-セッティングと同様の姿勢とし，非伸縮性バンドによる固定のない肢位とし矢印の方向に力を加えた．

c：SLR．背臥位で非測定足の膝を屈曲させ，膝伸展位で土面台から20°挙上した肢位とした．

d：膝伸展運動．坐位で伸展位とした．

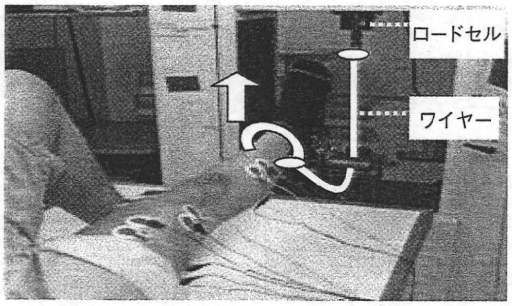

図3 オートグラフを用いたSLRの測定肢位
1kNロードセルに固定したワイヤーを足首に固定し挙上させて最大筋力測定および最大筋力の60%筋力を発揮させた．

膝関節を屈曲約30度とした長坐位で膝窩部に測定器を配置し，骨盤帯と下腿遠位部に非伸縮性バンドで固定した（図2a）．固定なしQ-セッティングは，固定ありQ-セッティングで同様の姿勢とし，非伸縮性バンドによる固定のない肢位とした（図2b）．SLRは，背臥位で非測定側の膝を屈曲させ，膝伸展位で土面台から20°挙上した肢位とした（図2c）．膝伸展運動は，坐位で伸展位とした（図2d）．

測定中に60%筋力発揮を維持させる方法として以下の方法を用いた．

固定ありQ-セッティング，固定なしQ-セッティングでは，測定器を用いて最大筋力を計測し，その後最大筋力に対する60%筋力を設定し，60%筋力発揮時の筋活動を計測した．本測定器は，設定した筋力発揮に対し，設定した負荷量に達した際に音と表示する機能をもつ[5]．

SLRでは，オートグラフを用い1kNロードセルに固定したワイヤーを足関節部に固定し挙上させ（図3），このときの最大引っ張り強度をSLR時の最大筋力とした．最大筋力に対する60%筋力を算出後，同様の肢位

で60%筋力を発揮させ，そのときの筋活動を計測した．SLRの計測は，表示される筋力値と指示により筋力発揮を行った．

60%筋力は，60%程度の筋力を維持させる状態として，予備実験により±10%程度のばらつきがあることを確認し，その範囲内のデータを有効とした．

膝伸展運動は，被験者に最大収縮を意識して発揮してもらった．

すべての訓練は，それぞれ設定条件で実施し，その訓練維持時間は10秒間とした．

6．統計処理

統計学的手法にはSPSS（ver. 11.5）を用いて，一元配置分散分析を行った．統計的有意水準は5%未満とした．

結　果

1．SLRの筋活動

7筋ともに膝伸展運動と同等の筋活動量であり，統計的な差は認められなかった．膝伸展運動に対する筋活動量は100～150%程度であった（図4）．

2．固定ありQ-セッティングの筋活動

前脛骨筋，腓腹筋およびハムストリングスでは，SLRおよび膝伸展運動の筋活動と統計的な差は認められなかった．大腿四頭筋ではすべての筋において最も筋活動量が高く，特に特に外側広筋，内側広筋では，SLR，膝伸展運動と比較して有意に高い筋活動量が確認された（$p<0.05$）（図4）．

3．固定なしQ-セッティングの筋活動

前脛骨筋，腓腹筋および大腿四頭筋では，

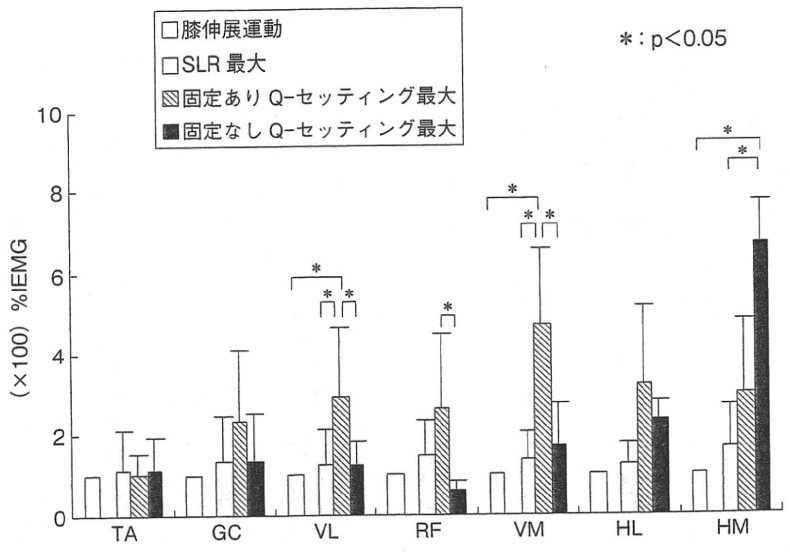

図4　部位別%IEMG

前脛骨筋（TA），腓腹筋（GC）について，訓練の違いによる筋活動の差は認められなかった．

外側広筋（VL），大腿直筋（RF），内側広筋（VM），外側ハムストリング（HL），内側ハムストリング（HM）について，固定ありQ-セッティングはSLR，膝伸展運動と比較して外側広筋，内側広筋で有意に高い筋活動が確認され（$p<0.05$），固定なしQ-セッティングはSLR，膝伸展運動と比較して内側ハムストリングで有意に高い筋活動が見られた（$p<0.05$）．

SLRおよび膝伸展運動の筋活動と統計的な差は認められなかった．内側ハムストリングではSLRおよび膝伸展運動と比較して有意に高い筋活動量が認められた（$p<0.05$）（図4）．

4．固定ありQ-セッティングと固定なしQ-セッティングの比較

固定することで内外側広筋，大腿直筋の筋活動量が有意に高くなった（$p<0.05$）（図4）．固定なしのQ-セッティングは内側ハムストリングの筋活動量が高くなった（$p<0.05$）（図5）．

5．同一負荷割合による比較

同一負荷割合（60%）における筋活動の違いは，固定ありQ-セッティングにおいては外側広筋が，固定なしQ-セッティングにおいては内側ハムストリングが他の訓練と比較して筋活動量が有意に高くなった（$p<0.05$）（図5）．また固定なしQ-セッティングの場合，SLRと比較して大腿直筋の筋活動が有意に低い結果となった．

考　察

本研究の結果から，膝伸展運動とSLRは類似の筋活動様式であったのに対し，Q-セッティングは，SLRおよび膝伸展運動とは異なる筋活動の様式を示した．固定ありQ-セッティングの場合，他の訓練と比較して大腿四頭筋のすべての筋で筋活動量が高く，特に広筋群で統計学的な有意差が認められた．これは固定することで骨盤および股関節の安定化が図られ主に膝伸展方向の力が働き，大腿四頭筋の筋出力が発揮しやすくなったためだと考えられる．固定なしQ-セッティングの場合，他の訓練と比較して大腿直筋の筋活動量が低い傾向にあったが大腿四頭筋全体としては差がないと考えられる．Soderbergら[6]やKarstら[2]はQ-セッティングは，SLRと比較すると内外側広筋の筋活動は高く，大腿直筋の筋活動は低いことを示しており，今回の結果でもほぼ同様の結果が得られた．

固定なしQ-セッティングは固定ありQ-セッティングとの比較において，外側ハムス

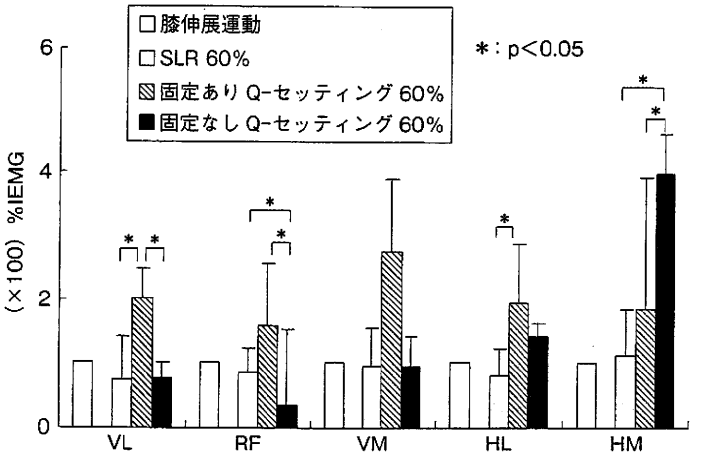

図5　60%負荷における%IEMG
固定ありQ-セッティングは外側広筋で，固定なしQ-セッティングは内側ハムストリングで他の訓練と比較して有意に筋活動が高い結果となった（$p<0.05$）．

トリングでは同等，内側ハムストリングでは有意に大きい筋活動であった．河村[4]は，股関節屈曲作用をもつ大腿直筋は股関節伸展が起きると働きが抑制されると述べていることから，固定なしQ-セッティングでは，この作用が働きハムストリングに影響を及ぼし，ハムストリングの拮抗二関節筋である大腿直筋の働きが抑制されたと考えられる．

以上のことから，Q-セッティングでは他の訓練と同等以上の効果があることが示され，方法を変えることで大腿四頭筋の筋活動を高め，またハムストリングの筋活動にも影響を及ぼすことが示唆された．

同負荷割合における筋活動の比較でも最大筋力発揮時とほぼ同様の結果で，固定ありQ-セッティングでは，外側広筋で筋活動が高く，固定なしQ-セッティングでは内側ハムストリングで筋活動が高くなった．この結果から，測定器を使用することで，強化したい筋を選択的に訓練することが可能であることが示唆された．

しかしながら，ハムストリングの筋活動が訓練効果のある大きさかどうかについては明確ではなく，今後ハムストリング単独の訓練などと固定なしQ-セッティングを比較し検証していく必要がある．さらに今回は，健康成人男女を対象とした研究報告であったが，下肢の筋力低下が顕著である高齢者や，変形性膝関節症を発症した患者においても同様の効果が得られるかを検証が必要と考える．

まとめ

測定器を用いたQ-セッティングは，膝伸展運動およびSLRと同等以上の筋活動が確認され，大腿前面の筋力トレーニング効果が期待できることが明らかとなった．さらに，固定なしのQ-セッティングでは，ハムストリングの筋活動に影響を及ぼすことを確認した．Q-セッティングにおいて固定の方法を変更することにより，効率的な強化または選択的に大腿四頭筋やハムストリングの訓練が可能であることが示唆された．

文　献

1) Baker KR. et al: The efficacy of home based progressive strength training in older adults with knee osteoarthritis: a randomized controlled trial. J Rheumatol. **28**(7): 1655-1665, 2001.
2) Karst GM. et al: Electromyographic analysis of exercises proposed for differential activation of medial and lateral quadriceps femoris muscle components. Phys Ther. **73**(5): 286-295, 1993.
3) 黒澤　尚ほか：変形性膝関節症に対するSLR訓練の効果―多施設RCTの結果―．日整会誌　**79**：9，2005.
4) 河村顕治：CKCにおける大腿直筋のサイレント現象とハムストリングの膝伸展作用．運動・物理療法　**20**：193，2009.
5) 縄田　厚ほか：セッティング式筋力測定・訓練機による膝伸展筋力と筋力発揮パターンの解析について．運動・物理療法　**19**：279-284，2008.
6) Soderberg GL. et al: Electromyographic analysis of knee exercises in healthy subjects and in patients with knee pathologies. Phys Ther. **67**(11): 1691-1696, 1987.
7) 渡辺博史ほか：大腿四頭筋セッティング訓練―視覚的なフィードバックの効果―．理学療法学　**28**：80，2001.
8) 渡辺博史：筋力強化の実際．古賀良生編，変形性膝関節症―病態と保存療法．南江堂，東京，pp 161-175，2008.

Journal of Surgical Oncology 2010;102:271–275

Clinical Outcomes of Minimally Invasive Surgery Using Acridine Orange for Musculoskeletal Sarcomas Around the Forearm, Compared With Conventional Limb Salvage Surgery After Wide Resection

TAKAO MATSUBARA, MD,[1,2] KATSUYUKI KUSUZAKI, MD,[3]* AKIHIKO MATSUMINE, MD,[1] HIROAKI MURATA, MD,[4] TOMOKI NAKAMURA, MD,[1] ATSUMASA UCHIDA, MD,[1] AND AKIHIRO SUDO, MD[1]

[1]Department of Orthopaedic Surgery, Mie Postgraduate School of Medicine, Tsu City, Mie Prefecture, Japan
[2]Department of Orthopaedic Surgery, Iga City Ueno Municipal Hospital, Iga, Mie Prefecture, Japan
[3]Department of Cell Physiology, Kyoto Prefectural Graduate School of Medical Science, Kyoto, Japan
[4]Department of Orthopaedic Surgery, Kyoto Prefectural University of Medicine, Kyoto, Japan

Background and Objectives: We recently developed and established a new surgical therapy combining photodynamic surgery and radiodynamic therapy using acridine orange (AO) therapy after marginal or intralesional tumor resection, providing excellent limb function to sarcoma patients. The present study evaluated local recurrence rate and limb function using Disability of Arm, Shoulder, and Hand (DASH) score of patients with primary musculoskeletal sarcoma around the forearm treated with AO therapy, compared to that of patients treated with conventional wide resection.

Methods: Subjects were 18 patients with primary musculoskeletal sarcoma around the forearm and treated with AO therapy (AO: n = 8) after marginal or intralesional resection, or conventional wide resection followed by limb reconstruction surgery (WR: n = 10).

Results: Mean age of the 18 patients was 45 years, and mean durations of follow-up for Groups AO and WR were 67 and 74.1 months. Local recurrence rates for AO and WR were 12.5% and 20% ($P = 0.63$), DASH disability scores were 3.9 and 21 ($P = 0.04$), and 5-year survival rates were 100% and 90% ($P = 0.40$), respectively.

Conclusions: AO therapy offers maintenance of excellent upper limb function and inhibition of local tumor recurrence, representing a useful modality for limb salvage surgery in patients with sarcoma around the forearm.

J. Surg. Oncol. 2010;102:271–275. © 2010 Wiley-Liss, Inc.

KEY WORDS: **hand and forearm sarcoma; acridine orange; photodynamic therapy; minimum invasive surgery; limb function**

INTRODUCTION

Although limb salvage surgery involving wide resection and limb reconstruction for musculoskeletal sarcomas is clearly well established and represents the most common approach, limb function is unsatisfactory for many patients, particularly those with sarcoma arising around the forearm and hand. In this site, wide resection of tumor is not easy and reconstructing good limb function is complicated by the major nerves and vessels with the small volume of muscles and skin. Patients thus frequently experience serious dysfunction of the hand and fingers after surgery, resulting in a useless limb that can contribute to mental depression and greatly reduced quality of life.

To avoid this scenario, we have recently established a new limb salvage strategy [acridine orange (AO) therapy] for minimally invasive surgery involving tumor excision with minimal margins, supported by photodynamic surgery (PDS), photodynamic therapy (PDT), and radiodynamic therapy (RDT) using AO in patients with high-grade malignant sarcoma [1–6]. The present study investigated the effectiveness of AO therapy in patients with sarcoma arising around the forearm and hand, compared with conventional limb salvage surgery.

MATERIALS AND METHODS

Subjects comprised patients who had undergone limb salvage surgery for primary bone and soft tissue sarcomas arising around the forearm involving the elbow and wrist joints between 1996 and 2008. All the patients had bone and soft tissue sarcomas which attached with nerve (radial, medial, or ulnar nerve), major vessels, or tendons. Operation notes were used to obtain the details of surgery. Pathology reports were consulted to identify the type, grade, and margins of the tumor. Disability of Arm, Shoulder, and Hand (DASH) scores were used to assess postoperative function in a postal survey [7]. Eighteen patients (12 men, 6 women) were recruited from the Departments of Orthopaedic Surgery at the University Hospital of the Kyoto Prefectural University of Medicine and Mie Postgraduate School of Medicine. Until 1999, we had performed conventional wide resection for primary high-grade sarcomas, followed by various limb reconstruction surgeries (Group WR, n = 10). From 1999, we attempted AO therapy for patients who would otherwise experience severe dysfunction of the elbow, wrist, hand, or fingers (Group AO, n = 8).

AO Therapy

All cases undergoing AO therapy received intralesional or marginal tumor excision, similar to conventional tumor excision for benign

Grant sponsor: Ministry of Education, Science, Sports and Culture o Japan; Grant number: 14207058.

*Correspondence to: Katsuyuki Kusuzaki, MD, Department of Cell Physiology, Kyoto Prefectural Graduate School of Medical Science, 465 Kajii-cho Kawaramachi-Hirokoji Kamigyo-ku, Kyoto 602-0841, Japan. Fax: +81-75-251-0295. E-mail: kusuzaki@koto.kpu-m.ac.jp

Received 21 October 2009; Accepted 30 March 2010

DOI 10.1002/jso.21602

Published online 24 May 2010 in Wiley Online Library (wileyonlinelibrary.com).

musculoskeletal tumors. These procedures were used to minimize damage to intact muscles and bones, as well as major nerves and vessels that were in close contact with the tumor and important to maintain excellent limb function.

For the next step involving AO–PDS, microscopic curettage was performed using an ultrasonic surgical scalpel (Olympus, Tokyo, Japan) in addition to using a fluorescence surgical microscope (Carl Zeiss, Oberkochen, Germany), under tumor fluorovisualization after local administration of 1 μg/ml of AO solution for 5 min, followed by washing out of excess AO solution with saline and excitation with blue light, which most effectively excites AO to emit green fluorescence [8]. AO binds densely to lysosomes and acidic vesicles especially in tumor cells immediately, and AO staining is useful for visual localization of the tumor during surgery under fluorescence microscope [1–3]. The microscope was equipped with an interference filter (450–490 nm) to select the blue light emitted by a xenon lamp, and an absorption filter (>520 nm) to allow for observation of the green AO fluorescence under fluorescence surgical microscopy. Microscopic curettage was repeated until green fluorescence had disappeared completely from the remnant tumor mass [1–6].

AO–PDT was subsequently applied to the area of tumor curettage under illumination with >100,000 1× of unfiltered light from the xenon lamp for 10 min, again using fluorescence surgical microscopy.

For cases in which the patient (n = 5) accepted low-dose radiotherapy (RT) after closure of the surgical wound without washing out the AO solution, AO–RDT was immediately performed using the following procedure. In the RT room, a single session of X-ray irradiation (5 Gy) was applied to the resected area to achieve a strong cytocidal effect of AO excited by low-dose X-rays [9].

Surgical margins were evaluated with pathology sections after operation in all 18 cases.

Statistical Analysis

Survival rate of patients and local recurrence rate were analyzed using Kaplan–Meier analysis. Upper limb function was evaluated using DASH disability criteria [7]. The main part of the DASH is a 30-item disability/symptom (DASH-DS) scale concerning the patient's upper extremity. These provide the DASH disability/symptom (DASHDS) score ranging from 0 (no disability) to 100 (the severest disability), after summation of the scores from all items and transformation. Functional evaluation was scored using DASH scale, and Student's *t*-test was used to assess for differences between the results of each condition. Significance is defined as $P < 0.05$.

This clinical trial was officially approved by the Ethics Committees of both participating Institutions. After a full explanation of the method and purposes of the study was given, each patient and a close family member provided written informed consent to participate in this clinical study.

RESULTS

Mean age of the 18 patients and histological diagnosis was shown in Table I. The 18 sarcomas were high-grade sarcomas. Mean durations of follow-up for Groups AO and WR were 67 months (range: 26–129 months) and 74.1 months (range, 35–141 months), respectively. In Group WR, patients were treated with wide margin resection, and four patients underwent limb reconstruction surgery using intraoperative irradiated autobone graft (RBG), skin flap and/or tendon transfer. Five patients were treated with pre- and postoperative chemotherapy and four patients received ordinary postoperative RT with high-dose X-ray (30–50 Gy total; Table II). In Group AO, tumors were resected with close margins to preserve limb function. Two osteosarcoma patients in Group AO underwent vascularized fibula autograft for forearm bone reconstruction. Three patients or their family members rejected AO–RDT due to the risk of complications after radiation, and these patients received only AO–PDS and PDT. Two of three patients who received only AO–PDS and AO–PDT had pre- and postoperative chemotherapy. Four patients treated with AO–RDT had pre- and postoperative chemotherapy (Table II). One patient with leiomyosarcoma underwent additional resection with AO therapy in our Institution at 1 month after intralesional tumor resection in other hospital.

As of September 2009, 7 of the 10 patients in Group WR were alive with continuous disease-free (CDF) status, 2 showed no evidence of disease (NED), and 1 had died of disease (DOD), due to pulmonary metastasis. Group AO showed 6 CDF patients, 2 NED patients, and no

TABLE I. Patient Distributions, Histological Diagnosis, Location, and AJCC Staging

Group	Sex		Age (years)		Follow-up (months)		Histological diagnosis		Location		AJCC stage soft tissue sarcomas (bone tumors)	
							Myxoid liposarcoma	2				
Wide resection (n = 10)	Male	7	Range	0–68	Range	35–141	Clear cell sarcoma	2	Elbow	1	I	0
	Female	3	Mean	46	Mean	74.1	MFH	2	Forearm	4	IIA	(1)
							Synovial sarcoma	1	Radius	2	IIB	3
							MPNST	1	Wrist	2	III	6
							Infantile fibrosarcoma	1	Hand	2	IV	0
							Chondrosarcoma	1				
							MFH	1				
AO therapy (n = 8)	Male	5	Range	19–82	Range	26–129	Synovial sarcoma	1	Forearm	5	I	0
	Female	3	Mean	46	Mean	67	Rhabdomyosarcoma	1	Radius	2	IIA	(1)
							Leiomyosarcoma	1	Hand	1	IIB	3
							Extraskeletal myxoid				III	3
							Chondrosarcoma	1			IV	(1)
							Fibrosarcoma	1				
							Periosteal osteosarcoma	1				
							Osteosarcoma	1				
Total	Male	12	Range	0–82	Range	26–141						
	Female	6	Mean	46	Mean	73.3						

AO, acridine orange; MFH, malignant fibrous histiocytoma; MPNST, malignant peripheral nerve sheath tumor; AJCC, Classification according to the American Joint Commission on Cancer criteria.

TABLE II. Pattern of Procedure, Adjuvant Therapy, and Outcome

	Pattern of procedure		Adjuvant therapy		Local recurrence	Survival (5 years)	Event-free (5 years)	DASH score
Wide resection	Wide resection		Pre- and postoperative		20% (n = 2)	90% (9/10)	70% (7/10)	1.7–56 (n = 9) Mean 21
	Wide resection + skin flap	2	Chemotherapy	5				
	Wide resection + RBG	1						
	Wide resection + RBG + tendon transfer	1	Radiotherapy	4				
AO therapy	PDS (intralesional) + PDT	1	Pre- and postoperative		12.5% (n = 1)	100% (8/8)	86% (7/8)	0–11 (n = 8) Mean 3.9
	PDS (marginal) + PDT	2	Chemotherapy	6				
	PDS (intralesional) + PDT + RDT	4						
	PDS (marginal) + PDT + RDT	1						
					$P = 0.63$	$P = 0.40$	$P = 0.38$	$P = 0.04^*$

RBG, intraoperative irradiated autobone graft; AO, acridine orange; PDS, photodynamic surgery; PDT, photodynamic therapy; RDT, radiodynamic therapy, DASH, Disability of the Arm, Shoulder and Hand criteria.
$^*P < 0.05$.

DOD patients. One osteosarcoma patient had already displayed pulmonary metastasis at diagnosis in our hospital.

Local recurrences rates were 12.5% in Group AO and 20% in Group WR ($P = 0.63$). Only 1 patient in Group AO showed local tumor recurrence, and this was the patient who had undergone intralesional resection in another hospital. For Group WR and Group AO, 5-year survival rates were 90% and 100% ($P = 0.40$), and 5-year event-free rates were 70% and 87.5% ($P = 0.38$), respectively. Seventeen of the 18 patients answered the DASH questionnaire, with one patient unable to answer because of a child. Mean DASH disability scores were 21 (Group WR) and 3.9 (Group AO; $P = 0.04$), respectively. Limb function in Group AO was much better than that in Group WR (Table II).

CASE PRESENTATION

Case 1 (Group WR)

The patient was a 69-year-old man with MFH arising in the right forearm (Fig. 1). The tumor was located beside the flexor digitorum and flexor carpi ulnaris (FCU) muscles. The tumor was resected with wide margins. FCU and flexor digitorum muscles of the little and ring fingers were resected with the tumor. The ulnar nerve was in close contact with the tumor, and thus was also resected (Fig. 2). However, postoperative histology of the resected tumor showed tumor positive results at part of the surgical margin. The patient therefore received conventional postoperative RT. Although no evidence of local recurrence has been seen as of 75 months after therapy, limb function of the hand and fingers was seriously poor (DASH score at end of follow-up, 33.3).

Case 2 (Group AO)

The patient was a 59-year-old man with MFH arising in the left forearm. Magnetic resonance imaging revealed tumor involvement with the extensor digitorum communis muscle (Fig. 3). The patient wished to preserve function of the hand and fingers, so we proposed AO therapy. After obtaining consent, marginal tumor resection followed by AO therapy with AO–PDS, PDT, and RDT was performed. Histologically, the tumor showed tumor-positive margins (Fig. 4). After 54 months, the tumor has not recurred and no metastases have been identified. DASH score for postoperative limb function was 0 and the patient has had no complaints about limb function.

DISCUSSION

High-grade malignant musculoskeletal sarcoma arising in the upper extremities is smaller and localized more superficially than that in the lower extremities. The prognosis of patients with tumor involving an upper extremity is better than that of patients with lower extremity tumor. However, local recurrence rates are higher for upper extremity sarcomas compared to those of the lower extremities, due to the small volume of muscles acting as a barrier against tumor invasion [10–12]. Particularly in sarcomas around the forearm, tumors frequently involve or invade major nerves such as the median, ulnar, and radial nerves, vessels such as the ulnar and radial arteries, and the numerous muscles, and tendons for finger and wrist motion. Conventional wide tumor resection with sacrifice of those structures is thus likely to cause severe dysfunction of the hand and fingers, markedly impacting activities of daily living and decreasing quality of life. To avoid such outcomes while inhibiting local tumor recurrence is obviously the ideal for patients, but is not easy.

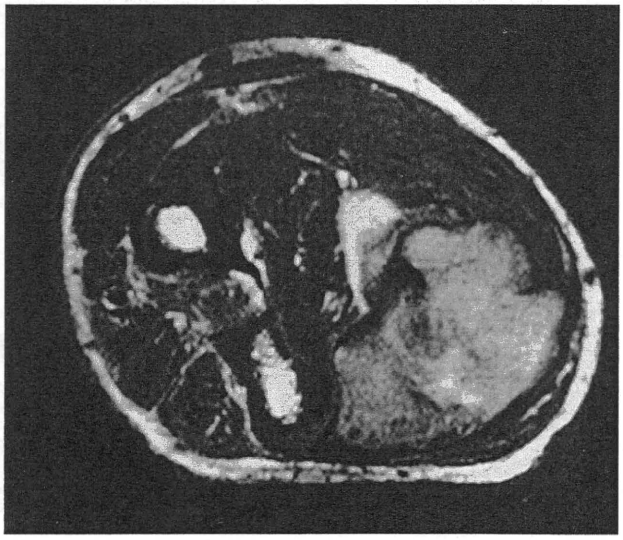

Fig. 1. MRI findings in Case 1 with MFH arising in the forearm. Axial T1-weighted imaging.

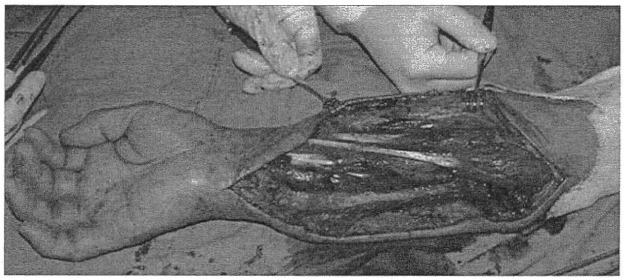

Fig. 2. Macroscopic findings of the operation in Case 1 showing the forearm after tumor resection with FDP, FCU, and ulnar nerve. [Color figure can be viewed in the online issue, available at wileyonlinelibrary.com]

We recently established the adjuvant modality of AO therapy using AO excited by photon energy for reduction surgery of high-grade malignant musculoskeletal tumors [1–6]. AO therapy consists of three main procedures: PDS, PDT, and RDT. During PDS, after the tumor is excised with an intralesional margin or marginal margin with minimal damage to normal tissues such as nerves, vessels, muscles, bones, and joints, AO solution is applied to the resected tumor area to expose the residual tumor mass to AO. Residual tumor emits green fluorescence originating from AO selectively binding to tumor cells, and this green fluorescence is readily visible under fluorescence microscopy. Since AO is retained much longer in malignant tumor cells than in normal cells, the green fluorescence is seen only in the tumor mass. Using an ultrasonic surgical knife, tumor emitting green fluorescence can be resected. Next, PDT is applied to the area in which surgery was performed. Moreover, if killing tumor cells that are covered or sealed with muscles is difficult, the RDT procedure irradiating 5 Gy of X-rays after surgery can also kill tumor cells situated deeply.

We have established the AO therapy methods described above based on the results of extensive experimental [8,13–17] and clinical trial studies [1–6]. This AO therapy method for limb salvage surgery is aimed not only at providing excellent limb function to patients with high-grade musculoskeletal sarcomas, but also at decreasing the risk of local recurrence.

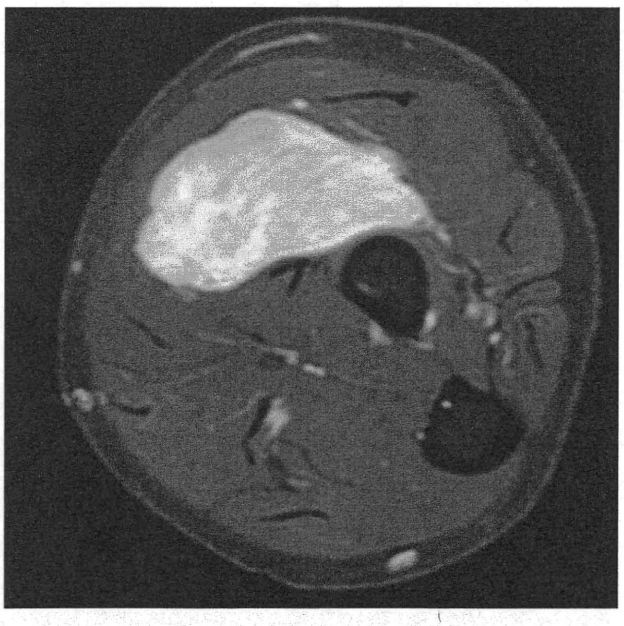

Fig. 3. Magnetic resonance imaging after preoperative chemotherapy in Case 2 with MFH arising in the forearm. Axial T1-weighted imaging.

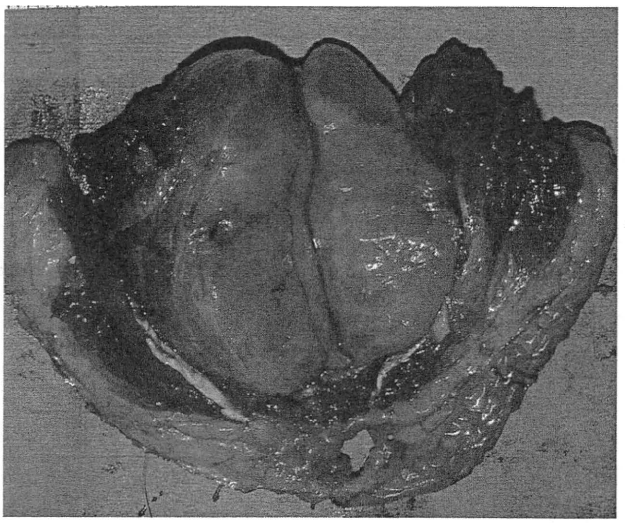

Fig. 4. Macroscopic findings of the resected tumor in Case 2. Marginal resection was performed. [Color figure can be viewed in the online issue, available at wileyonlinelibrary.com]

Clinical outcomes in the present study revealed that the results of Group WR versus Group AO were: local recurrence rate, 20% versus 12.5% ($P = 0.63$); 5-year survival rate, 90% versus 100% ($P = 0.38$); and 5-year event-free rate, 70% versus 86% ($P = 0.41$). These findings confirm that AO therapy is not inferior to wide resection in terms of local control and prognosis. In fact, AO therapy actually seems superior to wide resection from the perspective of clinical outcomes. Compared with previously published reports, local recurrence-free rate of AO therapy (87.5%) in the forearm was not inferior to that in the upper extremities (82%) [10]. In the Case 1 showing recurrence after AO therapy, the leiomyosarcoma had been excised with intralesional margins in another hospital. Tumor recurred in the ulnar bone marrow, not on the surface, after 17 months. We believe that recurrence developed as an intramedullary skip lesion that was difficult to treat with AO therapy without bone marrow curettage, since AO solution did not penetrate the cortical bone barrier.

Evaluation of limb function by DASH disability scoring showed vastly superior results for Group AO compared to Group WR. All patients who received AO therapy displayed excellent function of the elbow, hand, and fingers, as shown in Case 2, since AO therapy allows preservation of important muscles, nerves, and vessels. These clinical outcomes confirmed that AO therapy is useful for preserving excellent limb function in patients with high-grade sarcoma, particularly forearm and hand tumors that are close to important tissues for limb function.

In terms of margin status, significant correlations have been found between failure of local control and positive surgical margins in patients who undergo limb-conserving surgery and adjuvant RT [18]. Alektiar et al. [19] analyzed 110 patients with primary high-grade STS of the extremities with positive surgical margins, and 5-year local control rate was 74% in patients who received adjuvant RT, compared with 56% in patients treated with surgery alone. Adjuvant RT was thus suggested to improve local control in patients. Although our study included fewer cases than that study, local recurrence-free rate after marginal resection using AO therapy was better than that for adjuvant RT after inadequate surgery. Adjuvant RT frequently results in poor limb function, due to late fibrosis of soft tissues. AO–RDT with low-dose X-ray such as 5 Gy might thus offer a more effective means of controlling local recurrence and maintaining excellent limb function, compared with conventional adjuvant RT.

These clinical outcomes suggest that AO therapy might be useful for not only local tumor control, but also preservation of excellent limb function in high-grade malignant musculoskeletal tumors arising around the forearm. Of course, further studies involving larger numbers of patients and longer follow-up periods are needed.

CONCLUSIONS

AO therapy has potential as an excellent anticancer agent for limb salvage surgery, and AO therapy could represent a successful innovative surgical modality in cancer therapy.

ACKNOWLEDGMENTS

This work was supported in part by a Grant-in-Aid (14207058) for scientific research from the Ministry of Education, Science, Sports and Culture of Japan

REFERENCES

1. Kusuzaki K, Aomori K, Suginoshita T, et al.: Total tumor cell elimination with minimum damage to normal tissues in musculoskeletal sarcomas by photodynamic reaction with acridine orange. Oncology-Bazel 2000;59:174–180.
2. Kusuzaki K, Murata H, Matsubara T, et al.: Clinical trial of photodynamic therapy using acridine orange with/without low dose radiation as new limb salvage modality in musculoskeletal sarcomas. Anticancer Res 2005;25:1225–1235.
3. Kusuzaki K, Murata H, Matsubara T, et al.: Clinical outcome of a novel photodynamic therapy technique using acridine orange for synovial sarcomas. Photochem Photobiol 2005;81:705–709.
4. Yoshida K, Kusuzaki K, Matsubara T, et al.: Periosteal Ewing's sarcoma treated by photodynamic therapy with acridine orange. Oncol Rep 2005;13:279–282.
5. Kusuzaki K, Murata H, Matsubara T, et al.: Acridine orange could be an innovative anticancer agent under photon energy. In Vivo 2007;21:205–214.
6. Nakamura T, Kusuzaki K, Matsubara T, et al.: A new limb salvage surgery in cases of high-grade soft tissue sarcoma using photodynamic surgery, followed by photo- and radiodynamic therapy with acridine orange. J Surg Oncol 2008;97:523–528.
7. Imaeda T, Toh S, Nakao Y, et al.: Validation of the Japanese Society for Surgery of the Hand version of the Disability of the Arm, Shoulder and Hand Questionnaire. J Orthop Sci 2005;10: 353–359.
8. Ueda H, Murata H, Takeshita H, et al.: Unfiltered xenon light is useful for photodynamic therapy with acridine orange. Anticancer Res 2005;25:3979–3987.
9. Hashiguchi S, Kusuzaki K, Murata H, et al.: Acridine orange excited by low-dose radiation has a strong cytocidal effect on mouse osteosarcoma. Oncology-Bazel 2000;62:85–93.
10. Gerrand CH, Bell RS, Wunder JS, et al.: The influence of anatomic location on outcome in patients with soft tissue sarcoma of the extremity. Cancer 2003;97:485–492.
11. Trovik CS: Scanadinavian Sarcoma Group Project. Local recurrence of soft tissue sarcoma. A Scandinavian Sarcoma Group Project. Acta Orthop Scand Suppl 2001;72:1–31.
12. Sadoski C, Suit HD, Rosenberg A, et al.: Preoperative radiation, surgical margins, and local control of extremity sarcomas of soft tissues. J Surg Oncol 1993;52:223–230.
13. Kusuzaki K, Minami G, Takeshita H, et al.: Photodynamic inactivation with acridine orange on a multidrug-resistant mouse osteosarcoma cell line. Jpn J Cancer Res 2000;91:439–445.
14. Kusuzaki K, Suginoshita T, Minami G, et al.: Fluorovisualization effect of acridine orange on mouse osteosarcoma. Anticancer Res 2000;20:3019–3024.
15. Kusuzaki K, Murata H, Takeshita H, et al.: Intracellular binding sites of acridine orange in living osteosarcoma cells. Anticancer Res 2000;20:971–976.
16. Matsubara T, Kusuzaki K, Matsumine A, et al.: Acridine orange used for photodynamic therapy accumulates in malignant musculoskeletal tumors depending on pH gradient. Anticancer Res 2006;26:187–193.
17. Satonaka H, Kusuzaki K, Matsubara T, et al.: Extracorporeal photodynamic image detection of mouse osteosarcoma in soft tissues utilizing fluorovisualization effect of acridine orange. Oncology 2006;70:465–473.
18. Rosenberg SA, Tepper J, Glatstein E, et al.: The treatment of soft-tissue sarcomas of the extremities: prospective randomized evaluations of (1) limb-sparing surgery plus radiation therapy compared with amputation and (2) the role of adjuvant chemotherapy. Ann Surg 1982;196:305–315.
19. Alektiar KM, Velasco J, Zelefsky MJ, et al.: Adjuvant radiotherapy for margin-positive high-grade soft tissue sarcoma of the extremity. Int J Radiat Oncol Biol Phys 2000;48:1051–1058.

Biochemical and Biophysical Research Communications 400 (2010) 493–499

Contents lists available at ScienceDirect

Biochemical and Biophysical Research Communications

journal homepage: www.elsevier.com/locate/ybbrc

The cleavage of N-cadherin is essential for chondrocyte differentiation

Shigeto Nakazora [a], Akihiko Matsumine [a,*], Takahiro Iino [a], Masahiro Hasegawa [a], Ayae Kinoshita [b], Kengo Uemura [c], Rui Niimi [a], Atsumasa Uchida [a], Akihiro Sudo [a]

[a] Department of Orthopaedic Surgery, Mie University Graduate School of Medicine, 2-174, Edobashi, Tsu-city, Mie 514-8507, Japan
[b] Department of Health Sciences, Kyoto University Graduate School of Medicine, Yoshidakonoe-cho, Sakyo-ku, Kyoto, Japan
[c] Department of Neurology, Kyoto University Graduate School of Medicine, 53 Shogoinkawahara-cho, Sakyo-ku, Kyoto, Japan

ARTICLE INFO

Article history:
Received 10 August 2010
Available online 22 August 2010

Keywords:
N-cadherin, Ectodomain shedding
Extracellular matrix protein
Chondrocyte differentiation
ATDC5

ABSTRACT

The aggregation of chondroprogenitor mesenchymal cells into precartilage condensation represents one of the earliest events in chondrogenesis. N-cadherin is a key cell adhesion molecule implicated in chondrogenic differentiation. Recently, ADAM10-mediated cleavage of N-cadherin has been reported to play an important role in cell adhesion, migration, development and signaling. However, the significance of N-cadherin cleavage in chondrocyte differentiation has not been determined. In the present study, we found that the protein turnover of N-cadherin is accelerated during the early phase of chondrogenic differentiation in ATDC5 cells. Therefore, we generated the subclones of ATDC5 cells overexpressing wild-type N-cadherin, and two types of subclones overexpressing a cleavage-defective N-cadherin mutant, and examined the response of these cells to insulin stimulation. The ATDC5 cells overexpressing cleavage-defective mutants severely prevented the formation of cartilage aggregates, proteoglycan production and the induction of chondrocyte marker gene expression, such as type II collagen, aggrecan and type X collagen. These results suggested that the cleavage of N-cadherin is essential for chondrocyte differentiation.

1. Introduction

Cartilage formation in the developing vertebrate embryonic limb consists of a highly coordinated and orchestrated series of events involving mesenchymal cell recruitment, migration, proliferation and condensation, which are regulated by mesenchymal–epithelial cell interactions [1–3]. The aggregation of chondroprogenitor mesenchymal cells into precartilage condensations represents one of the earliest events in chondrogenesis [2,4]. For the condensation of chondroprogenitor mesenchymal cells, cell–cell adhesion through molecules such as neural cadherin (N-cadherin), neural cell adhesion molecule (N-CAM), and tenascin C are required [5,6]. In these molecules, N-cadherin has been reported to be a key cell adhesion molecule implicated in chondrogenic differentiation.

N-cadherin, named for its initial identification in neural tissue, was one of the first identified cadherins and its functional involvement in cell–cell adhesion and development has been extensively studied. N-cadherin is one of the Ca^{2+}-dependent adhesion molecules and it is a member of the cadherin superfamily, which is divided into six subgroups based on structural similarities. Its large N-terminal extracellular domain is composed of five tandem repeat domains, termed cadherin repeats, that contain four Ca^{2+}-binding sites, and are involved in homotypic protein–protein interactions, maintaining the extracellular domain in a stiff, rod-like conformation (Fig. 1A) [7–11]. The conserved cytoplasmic domain is responsible for binding to the actin cytoskeleton through the catenin family of proteins [12,13].

Recently, cadherin cleavage has been intensively studied because it controls both cell–cell adhesion by regulating the amount of cadherin as well as the extracellular and intracellular signal transduction arising from the cadherin molecule. It was demonstrated that N-cadherin can be first cleaved by a disintegrin and metalloproteinase-10 (ADAM-10) protein at the extracellular domain [14–16]. Cleavage of N-cadherin at the extracellular domain produces ectodomain soluble fragment which can act as extracellular signaling molecule-like growth factors, and Ncad/C-terminal fragment 1 (CTF1), a membrane fragment. Thereafter, presenilin1 (PS1)/γ-secretase-mediated cleavage of N-cadherin at the intracellular domain produces Ncad/C-terminal fragment 2 (CTF2) (Fig. 1A). The ectodomain shedding, which disrupts cell–cell contacts, is a prerequisite for the secondary PS1/γ-secretase cleavage [14]. Although N-cadherin and β-catenin form a complex beneath the plasma membrane stabilizing cell–cell contacts, presenilin1 (PS1)/γ-secretase-mediated cleavage of N-cadherin promotes the nuclear translocation of β-catenin, and leads to enhanced transcriptional nuclear signaling [15,17]. Therefore, N-cadherin fragments formed by these sequential proteolytic events are considered to be a crucial molecule that switches the signal of cell–cell adhesion to that of cell proliferation or cell differentiation.

* Corresponding author. Fax: +81 59 231 5211.
E-mail address: matsumin@clin.medic.mie-u.ac.jp (A. Matsumine).

0006-291X/$ - see front matter © 2010 Elsevier Inc. All rights reserved.
doi:10.1016/j.bbrc.2010.08.070

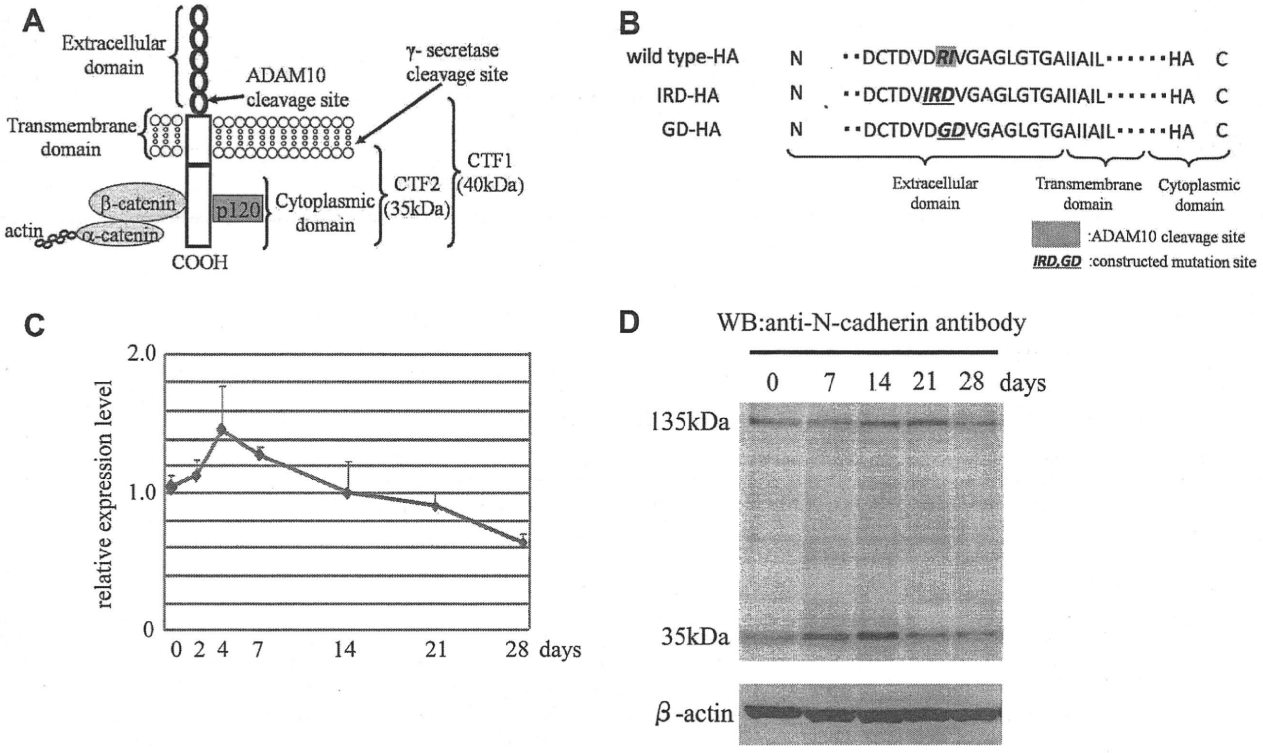

Fig. 1. Structure of N-cadherin protein and ADAM10-mediated cleavage-defective mutants of N-cadherin, and expression N-cadherin in ATDC5 cells. (A) A schematic drawing of the N-cadherin cleavage sites. Full-length 135-kDa N-cadherin is cleaved by ADAM10, producing N-terminal 95-kDa fragments and C-terminal 40-kDa fragments (CTF1). CTF1 is further processed by PS1/γ-secretase, creating 35-kDa fragments (CTF2). (B) A schematic drawing of the N-cadherin mutants. The putative cleavage site was located between R^{714} and I^{715} in the extracellular domain of wild-type N-cadherin (checked sheet). We generated the following two cleavage-defective mutants of N-cadherin by site-directed mutagenesis: the IRD mutant, containing D713I and I715D, and the GD mutant, containing R714G and I715D (underlined). All constructs were tagged with HA at the C-terminus. (C) After the induction of chondrogenic differentiation by insulin stimulation, the expression levels of N-cadherin mRNA were upregulated at day 4, and gradually decreased thereafter. (D) The full-length N-cadherin (135 kDa) protein was expressed at a constant level, and N-cadherin cleavage was increased 2–3-fold between days 7 and 14 during chondrogenic differentiation. These results suggested that the protein turnover of N-cadherin is accelerated during the early phase of chondrogenic differentiation in ATDC5 cells.

However, the significance of N-cadherin cleavage underlying chondrocyte differentiation has not been clearly examined. The purpose of the present study is to explore the significance of N-cadherin cleavage in chondrogenic differentiation.

2. Material and methods

2.1. Construction of N-cadherin mutant expression vector

A cDNA copy of the human N-cadherin (Genbank No.: M34064) gene was amplified from the first strand cDNA from human fetal brain (Stratagene, CA), and was thereafter cloned into pcDNA3.1 (+) (Invitrogen, Carlsbad, CA) as we previously described [14]. For C-terminal HA-tagging, the reverse primer 5'-TTTTTGGGCCCTCAG GCGTAATCTGGGACGTCGTATGGGTAGTCATCACCTCCACCATACATG TCAGCA-3' was used. Uemura et al. demonstrated that ADAM10-mediated cleavage of N-cadherin occurs between R^{714} and I^{715} in the extracellular domain [14]. Therefore, we used the following two cleavage-defective mutants of N-cadherin generated by the site-directed mutagenesis: the GD mutant containing R714G and I715D, and the IRD mutant with D713I and I715D (Fig. 1B) [14].

2.2. Cell culture

The mouse embryonal carcinoma-derived chondrogenic cell line ATDC5 was purchased from Cell Bank, RIKEN BioResource Center (Ibaraki, Japan). ATDC5 cells were cultured as we previously described [18]. For the induction of chondrogenesis, human recombinant insulin (Roche Diagnostics, Tokyo Japan) was added to a final concentration of 10 μg/ml in medium. To generate cell clones stably expressing N-cadherin or an N-cadherin mutant, constructs were transfected into ATDC5 cells using Lipofectamine 2000 and OPTI-MEM (Invitrogen, Tokyo, Japan), followed by culture in selection medium containing 500 ng/ml G418 (Nacalai Tesque, Kyoto, Japan). To maintain the expression of N-cadherin, we used a maintenance medium containing 300 ng/ml G418. To generate control clones of stable transfectants without N-cadherin insert (mock), pcDNA3.1 vector was transfected into ATDC5 cells. The cell morphology was analyzed using microscopy: OLYMPUS BX50 (Olympus Co., Tokyo, Japan) and recorded with a digital color camera: OLYMPUS DP-70 (Olympus Co., Tokyo, Japan).

2.3. Antibodies

A mouse monoclonal antibody to N-cadherin was purchased from BD Transduction Laboratories Inc. (CA, USA). A mouse monoclonal antibody to the HA-tag and mouse monoclonal anti-β-actin antibody were purchased from Sigma–Aldrich (Tokyo Japan). The polyclonal anti-ADAM10 antibody was obtained from Chemicon (Temecula, CA) and Calbiochem (Merk, Tokyo, Japan). As the secondary antibody of Western blot, horseradish peroxidase-conjugated anti-mouse and anti-rabbit IgG antibodies (GE Healthcare UK Ltd., Buckinghamshire, England) were used.

2.4. Western blot analysis

We performed the Western blot analyses using whole-cell lysates which were collected from 5×10^5 cells as we previously de-

scribed [18]. The bands were visualized using the ECL Western blotting detection system (GE Healthcare UK Ltd., Buckinghamshire, England) and were detected by LAS-4000 (Fujifilm, Tokyo, Japan).

2.5. Alcian blue staining

To investigate the synthesis of the proteoglycan production, we performed Alcian blue staining of the cultured ATDC5 cells. Each cell line was plated at a cell density of 6×10^4 cells per well of 6-well plates (BD FALCON, Tokyo, Japan) in the maintenance medium. After the cultures reached confluency, human insulin (10 μg/ml) was added to the medium to induce chondrogenesis (day 0). The plates were washed two times with PBS. Thereafter, the cell layers were fixed with 95% methanol at −20 °C for 2 min, and stained with 0.1% Alcian Blue (Muto Pure Chemicals Co., Ltd., Tokyo, Japan) as we previously described [18]. To obtain the quantitative data, the dye was extracted with 6 M guanidine-HCl for 18 h, and the total optical density of extracted dye was measured using a spectrophotometer (Thermo Fisher Scientific K.K., Yokohama, Japan) at 620 nm and designated as A_{620}.

2.6. Total RNA extraction and quantitative real-time polymerase chain reaction

Each cell line was plated as described, and the cells were harvested. After washing each plate three times with cold PBS, the total RNA was extracted from ATDC5 cells as we previously described [18]. TaqMan Universal PCR Master Mix and TaqMan Gene Expression Assays for genes including N-cadherin, β-actin, type II collagen, type X collagen, and aggrecan were purchased from Applied Biosystems (CA, USA). Real-time quantitative PCR amplification was performed on the ABI PRISM 7000 Sequence Detection System (Applied Biosystems, CA, USA). β-Actin was used as an endogenous reference gene for normalization. Standard curves were generated using cDNA samples from ATDC5-mock on day 14 after induction of chondrogenic differentiation. The relative expression levels of each target gene were indicated by calculating the ratio for those from ATDC5-mock on day 14. All assays were performed in triplicate and repeated three times.

2.7. Immunofluorescence

ATDC5 cells transiently transfected with constructs were stimulated by insulin on day 2, and fixed with methanol at −20 °C for 10 min on day 5. And they were blocked with 3% BSA in PBS for 15 min, and incubated with a mouse monoclonal antibody to the HA-tag (Sigma–Aldrich, Tokyo Japan) for 1 h at room temperature, washed three times with PBS containing 0.2% BSA, and incubated with AlexaFlour488-conjugated goat anti-mouse IgG(H + L) (Invitrogen, Tokyo, Japan). Microscopic signals were recorded using a confocal laser scanning microscope, Fluoview FV1000 (Olympus Co., Tokyo, Japan).

3. Results

3.1. Detection of the cleavage of N-cadherin during the chondrogenic differentiation of ATDC5 cells

To investigate the significance of N-cadherin in chondrogenic differentiation, we used ATDC5 cell line. ATDC5 cells are clonal mouse embryonic carcinoma cells that display a number of characteristics of committed chondroprogenitor cells and undergo insulin-induced chondrocyte differentiation, which resembles chondrocyte differentiation *in vivo* [18].

First, we examined N-cadherin expression by quantifying the levels of N-cadherin mRNA. After induction of chondrogenic differentiation with insulin stimulation, the expression level of N-cadherin was upregulated at day 4, and gradually decreased thereafter (Fig. 1C).

Next, we investigated N-cadherin protein expression and found that full-length N-cadherin protein was constantly expressed during chondrogenic differentiation, in spite of drastic induction of the N-cadherin mRNA levels (Fig. 1D). Interestingly, the cleavage of N-cadherin was increased 2–3-fold between days 7 and 14. These results suggested that protein turnover of N-cadherin, which is composed of both protein production and degradation, is accelerated during the early phase of chondrogenic differentiation in ATDC5 cells.

3.2. Isolation of subclones of ATDC5 cells overexpressing wild-type N-cadherin or cleavage-defective N-cadherin

As previous reports indicated that cleavage of N-cadherin is mediated by ADAM10 [14,15], we examined the expression of ADAM10 in ATDC5 cells, and observed the 85-kDa band corresponding to ADAM10 (Fig. 2A). To investigate the biological significance of ADAM10-mediated cleavage of N-cadherin in chondrocyte differentiation, we first generated HA-tagged N-cadherin mutant gene constructs by the site-directed mutagenesis: the GD mutant and IRD mutant (Fig. 1B). Thereafter, we isolated the subclones of ATDC5 cell lines: ATDC5-mock which is stable transfectant of pcDNA3.1 vector, ATDC5-NCAD(WT) which stably overexpress wild-type N-cadherin, and ATDC5-NCAD(GD) and ATDC5-NCAD(IRD), expressing cleavage-defective mutants of N-cadherin.

Next, to confirm whether overexpressed N-cadherin protein in ATDC5-NCAD(GD) and ATDC5-NCAD(IRD) cells is cleaved, a Western blot analysis was performed on the cell lysates (Fig. 2B). The cytoplasmic HA-tag immunoreactivity of CTF2 produced by the cleavage of N-cadherin was observed only in ATDC5-NCAD(WT) cells, at a molecular weight of 35 kDa. In ATDC5-NCAD(GD) and ATDC5-NCAD(IRD) cells, there were no bands that corresponded to CTF2. These results suggest that the two types of mutant N-cadherin protein derived from the NCAD(GD) and NCAD(IRD) cells are ADAM10-cleavage-deficient. Thereafter, we compared the cell morphology among the clones. When the cells were in the logarithmic growth phase without cell–cell contacts, there were no specific differences observed between the clones (data not shown). However, 7 days after the induction of chondrocyte differentiation, there were drastic morphologic distinctions among the 4 ATDC5 subclones. As shown in Fig. 2C–F, the ATDC5-mock cells underwent progressive differentiation over the 28-day period in medium containing insulin, as shown by increased cell condensation. In contrast, the ATDC5-NCAD(WT) cells showed decreased condensation, and ATDC5-NCAD(GD) and ATDC5-NCAD(IRD) cells revealed the complete absence of cell condensation.

3.3. The effect of overexpression of the wild-type and ADAM10-mediated cleavage-deficient forms of N-cadherin on cartilage nodule formation and proteoglycan production.

To determine the functional effect of N-cadherin cleavage on chondrocyte differentiation, we examined the cartilage nodule formation and proteoglycan production in ATDC5-mock, ATDC5-NCAD (WT), ATDC5-NCAD (GD) and ATDC5-NCAD (IRD) cells. As shown in Fig. 3A, ATDC5-mock and ATDC5-NCAD(WT) cells underwent progressive differentiation over the 21-day period in insulin-containing medium, as observed by the increased formation of cartilage aggregates and increased Alcian blue staining beginning at day 14, while the extent of staining in ATDC5-NCAD(WT) cells was weaker than that of ATDC5-mock cells. In

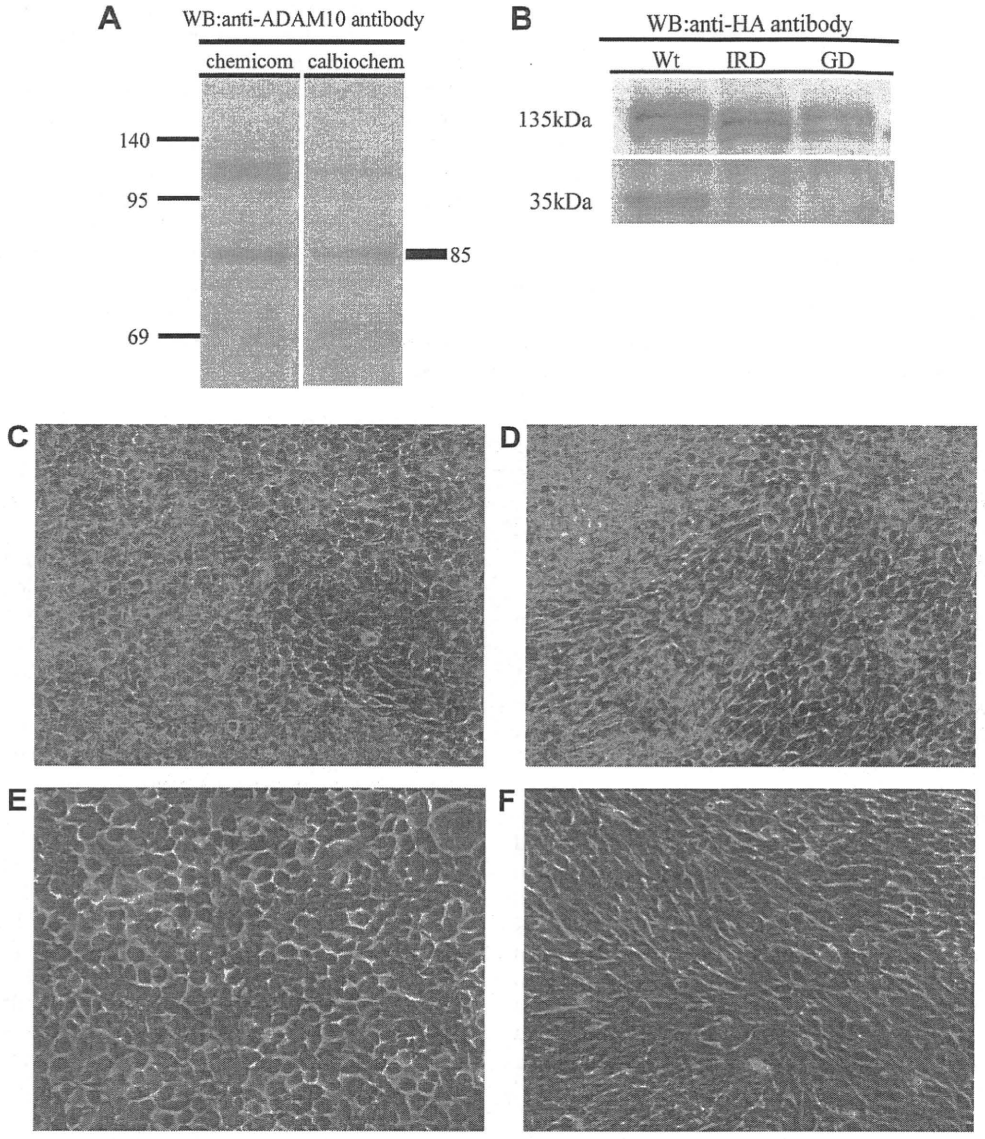

Fig. 2. (A) The expression of ADAM10 in ATDC5 cells. The band at the level of 85 kDa corresponded to ADAM10 and was identified with two independent antibodies. (B) A Western blot analysis of ATDC5-NCAD(WT) expressing wild-type N-cadherin, and ATDC5-NCAD(GD) and ATDC5-NCAD(IRD) cells overexpressing cleavage-defective mutants. The HA-tag immunoreactivity of CTF2 produced by the cleavage of N-cadherin was observed only in ATDC5-NCAD(WT) cells at a molecular weight of 35 kDa. There was no band corresponding to CTF2 in the ATDC5-NCAD(GD) or ATDC5-NCAD(IRD) cell lysates. Microscopic findings of (C) ATDC5-mock, (D) ATDC5-NCAD(WT), (E)ATDC5-NCAD(GD) and (F) ATDC5-NCAD(IRD) cells. The ATDC5-mock cells showed cell condensation over the 28-day period in medium containing insulin. In contrast, the ATDC5-NCAD(WT) cells showed decreased condensation, and ATDC5-NCAD(GD) and ATDC5-NCAD(IRD) exhibited no cell condensation.

contrast, ATDC5-NCAD(GD) and ATDC5-NCAD(IRD) cells exhibited considerably decreased Alcian blue staining compared to ATDC5-mock and ATDC5-NCAD(WT) cells. A quantitative determination of the extent of proteoglycan production showed that the Alcian blue staining in ATDC5-NCAD(WT) cells was partially suppressed in comparison to that in ATDC5-mock cells (Fig. 3B). In ATDC5-NCAD(GD) and ATDC5-NCAD(IRD) cells, the extent of staining was completely suppressed. These results suggested that the inhibition of the N-cadherin cleavage suppressed cartilage aggregate formation and proteoglycan production in ATDC5 cells.

3.4. The effect of an overexpression of wild-type and ADAM10 mediated cleavage-deficient form of N-cadherin on chondrocyte differentiation at the molecular level

The effect of an overexpression of wild-type and cleavage-defective mutants of N-cadherin on chondrocyte differentiation at the molecular level was examined by quantifying the expression levels of the chondrocyte marker genes, including type II collagen, aggrecan, and type X collagen. As a result, the cleavage-defective mutants were found to severely prevent the expression of type II collagen, aggrecan and type X collagen during insulin-induced differentiation, while ATDC5-mock cells exhibited upregulation of type II collagen and aggrecan, which peaked on day 14 (Fig. 3C–E). However, ATDC5-NCAD(WT) cells exhibited partial suppression of these chondrocyte marker genes during insulin-induced differentiation. These results suggested that the cleavage of N-cadherin is essential for chondrocyte differentiation.

3.5. Subcellular localization of N-cadherin protein

To investigate the mechanism of inhibition of chondrogenic differentiation in ATDC5 cells overexpressing cleavage-defective mutants of N-cadherin, we examined the subcellular location of N-cadherin after induction of chondrogenic differentiation. In ATDC5-NCAD(WT) cells, N-cadherin was observed in the cyto-

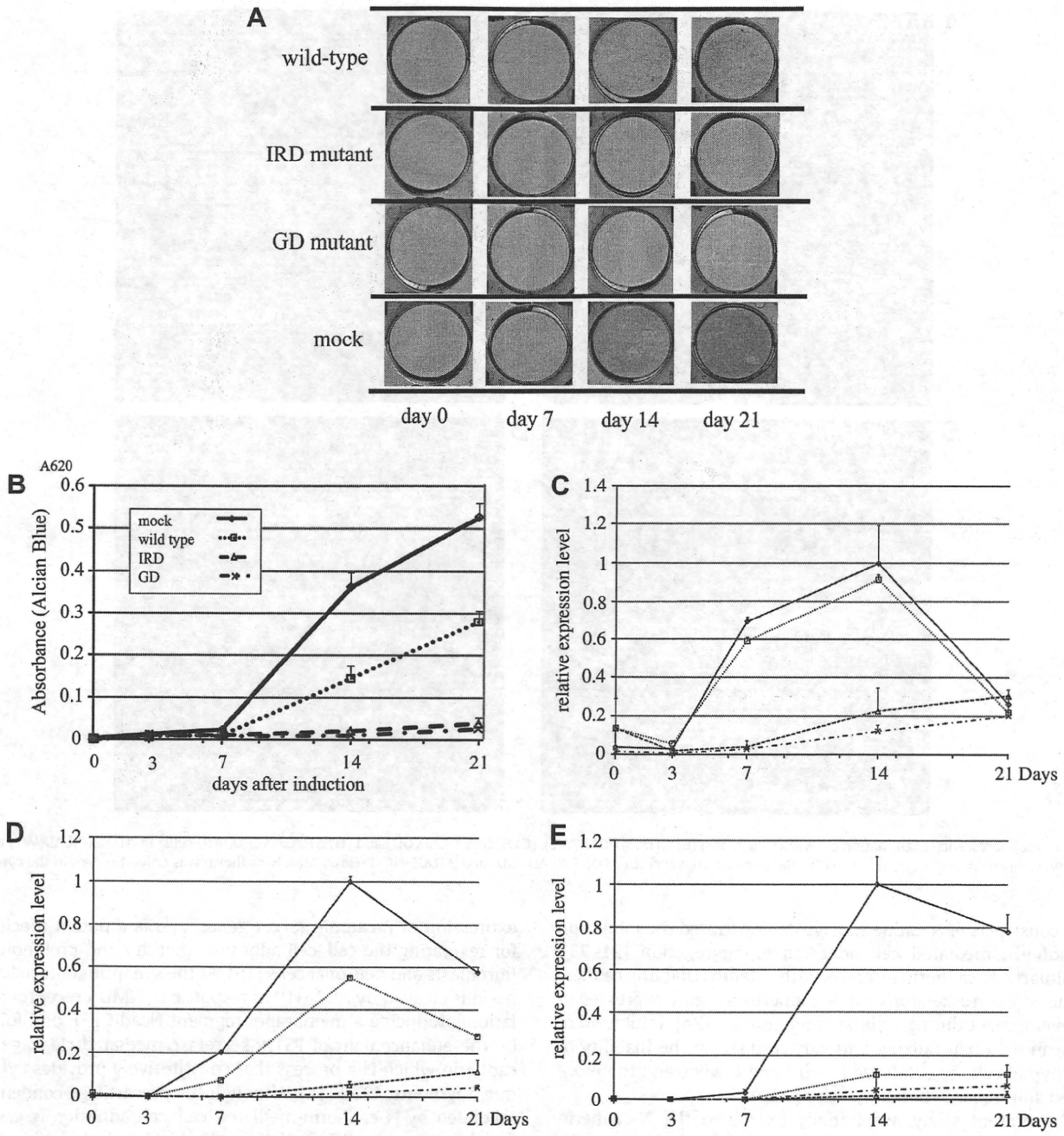

Fig. 3. The effect of an overexpression of wild-type N-cadherin and its cleavage-defective mutants on proteoglycan production (A) ATDC5-mock cells underwent progressive chondrogenic differentiation in medium containing insulin, as evidenced by the increased formation of cartilage aggregates and Alcian blue staining beginning at day 14. In contrast, the GD- and IRD-expressing cells were not stained by Alcian blue, and did not form cartilage aggregates. Cells overexpressing wild-type N-cadherin exhibited mild staining. (B) In the quantitative measurement of proteoglycan production, the cleavage-defective mutants exhibited nearly complete suppression of Alcian blue staining during the induction of chondrogenesis. Furthermore, cleavage-defective mutants almost completely prevented the induction of (C) type II collagen (D) aggrecan and (E) type X collagen expression during insulin-induced differentiation, while ATDC5-mock cells did not have altered expression of these three genes. ATDC5-NCAD(WT) cells exhibited partially suppressed type II collagen and aggrecan expression, but strongly suppressed type X collagen gene expression (open diamonds: ATDC5-mock, open squares: ATDC5-NCAD(WT), open triangles: ATDC5-NCAD(IRD), X: ATDC5-NCAD(GD)).

plasm and in the nucleus (Fig. 4B). However, in ATDC5-NCAD(GD) and ATDC5-NCAD(IRD) cells, N-cadherin was observed only in the cytoplasm (Fig. 4C and D).

4. Discussion

The process of chondrogenesis occurs in stages, beginning with mesenchymal cell recruitment and migration, proliferation and condensation, which are regulated by mesenchymal–epithelial cell interactions. The aggregation of chondroprogenitor mesenchymal cells into precartilage condensations represents one of the earliest events in chondrogenesis [1–4]. For the condensation of chondroprogenitor mesenchymal cells, cell–cell adhesion through molecules such as neural cadherin (N-cadherin), neural cell adhesion molecule (N-CAM), and tenascin C are required [1–5].

N-cadherin is a member of the classical cadherin family, and it binds in a hemophilic, calcium-dependent manner [19,20]. C3H10T1/2 cells, epithelial cells and L-cells expressing deletion

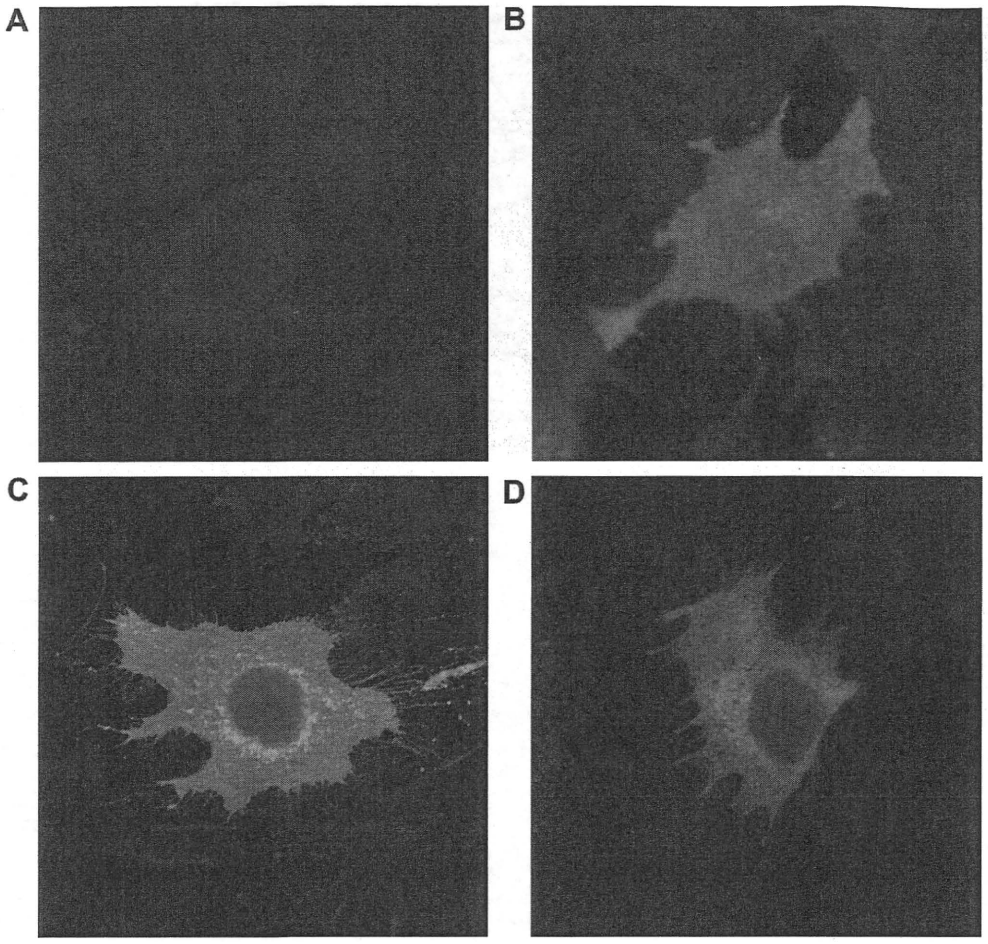

Fig. 4. Immunofluorescence examination of (A) ATDC5-mock, (B) ATDC5-NCAD(WT), (C) ATDC5-NCAD(GD) and (D) ATDC5-NCAD(IRD) cells. In ATDC5-NCAD(WT) cells, N-cadherin was observed in the cytoplasm and in the nucleus. However, in ATDC5-NCAD (GD) and ATDC5-NCAD (IRD) cells, N-cadherin was only observed in the cytoplasm.

mutant constructs of N-cadherin have demonstrated the inhibition of N-cadherin mediated cell adhesion or aggregation [21–23]. Intracellularly, N-cadherin interacts with catenins that link cadherins to the actin cytoskeleton [10]. N-cadherin is highly expressed in limb development during cellular condensation [24]. Inhibition of N-cadherin by a neutralizing antibody resulted in the inability of mesenchymal cells to condense *in vitro* and *in vivo*, and therefore inhibited subsequent chondrogenesis [24].

In the present study, we initially examined the N-cadherin expression in ATDC5 cells after the induction of chondrogenic differentiation by insulin stimulation, and observed that full-length N-cadherin was expressed at a constant level during chondrogenic differentiation, in spite of a drastic induction of the N-cadherin mRNA that peaked at day 4. And we found that CTF2, which is produced by the cleavage of N-cadherin, increased 2–3-fold between days 7 and 14. These results suggest that protein turnover of N-cadherin is accelerated during the early phase of chondrogenic differentiation in ATDC5 cells.

Recently, the proteolytic cleavage of various cell surface proteins such as growth factors, receptors and their ligands, cytokines, and cell adhesion molecules has attracted attention as a biological phenomenon which regulates cell adhesion, migration, development and signaling events [16]. In the case of N-cadherin, ADAM10-mediated proteolytic cleavage yields increased levels of the soluble N-cadherin fragment, which inhibits normal N-cadherin function in cellular adhesion [15]. ADAM10-mediated cleavage of N-cadherin induces the dramatic redistribution of β-catenin from the cell surface to the cytoplasmic pool, thereby inducing the expression of β-catenin target genes, and is a potent mechanism for regulating the cell–cell adhesion, motility and proliferation in fibroblasts and neuronal cells [15]. At the synaptic contacts, N-cadherin is cleaved by ADAM10 in response to NMDA receptor stimulation, producing a membrane fragment Ncad/CTF1, and followed by the enhancement of PS1/γ-secretase-mediated cleavage of N-cadherin which is a process that constitutively provides cytoplasmic fragments, CTF2 [14]. Although the precartilage condensation mediated by N-cadherin-mediated cell–cell adhesion is essential for chondrogenic differentiation, the biochemical significance of cleavage of N-cadherin in chondrocyte differentiation is not fully understood.

Thereafter, we showed that ADAM10, which cleaves the extracellular domain of N-cadherin, is expressed in ATDC5 cells. Previous reports also described the expression of ADAM10 in cartilaginous tissue during the continuous remodeling of human cartilage in newborns [25] and in the superficial chondrocytes of rat articular cartilage [26].

Next, to determine the significance of the cleavage of N-cadherin in chondrocyte differentiation, we generated four stable subclones in ATDC5 cells: ATDC5-mock, ATDC5-NCAD(WT), overexpressing wild-type N-cadherin; and ATDC5-NCAD (GD) and ATDC5-NCAD (IRD), which overexpress cleavage-defective N-cadherin mutants. We found that inhibition of N-cadherin cleavage suppressed cartilage aggregate formation and proteoglycan production during chondrocyte differentiation in ATDC5 cells. Moreover, the cleavage-defective mutants severely prevented the induction of genes such as type II collagen, aggrecan and type X

collagen. Therefore, the cleavage of N-cadherin was found to be essential for chondrocyte differentiation. It was recently reported that TGF-β3 downregulates ADAM 10 and inhibits cell proliferation and subsequent precartilage condensation by inhibiting the cleavage of N-cadherin in chick leg bud mesenchymal cells [27]. Our result is the direct verification which shows the significance of proteolytic cleavage of N-cadherin in chondrocyte differentiation.

To investigate the mechanism of inhibition of chondrogenic differentiation in ATDC5 cells overexpressing cleavage-defective mutants of N-cadherin, we examined the subcellular localization of N-cadherin in ATDC5 cells. We found that N-cadherin was observed both in the cytoplasm and in the nucleus in ATDC5-NCAD(WT) cells. However, in cleavage-defective mutant cells, N-cadherin was observed only in the cytoplasm. Le et al. reported that surface E-cadherin is actively internalized and recycled back to the plasma membrane [28]. Therefore, we considered that N-cadherin, which was observed in the cytoplasm, was actively internalized by endocytosis. Recently, Haas et al. [17] described the proteolytic fragment gamma-protocadherins, generated by gamma-secretase can localize to the nucleus. In the present study, N-cadherin was observed in the nucleus of ATDC5-NCAD(WT) cells, but not observed in the nucleus in ATDC5-NCAD (GD) and ATDC5-NCAD (IRD) cells. These results suggest that N-cadherin, observed in the nucleus of ATDC5-NCAD(WT) cells, consist of CTF2 that translocated from the cytoplasm to the nucleus after proteolytic cleavage. We speculated that the inhibition of chondrocyte differentiation by the overexpression of cleavage-defective mutants was due to the over-stabilization of hemophilic intercellular binding and to the absence of signal transduction by CTF2 from the cell surface receptor, N-cadherin. Further investigations are expected to clarify these hypotheses in the future.

5. Conclusion

We found that the protein turnover of N-cadherin is accelerated during the early phase of chondrogenic differentiation. Therefore, we examined the significance of cleavage of N-cadherin in chondrocyte differentiation by generating cleavage-defective mutants. ATDC5 cells overexpressing cleavage-defective mutants strongly prevented cartilage aggregate formation, proteoglycan production and the induction of chondrocyte marker genes, including type II collagen, aggrecan and type X collagen, following insulin stimulation. The inhibition of chondrocyte differentiation in ATDC5 cells with cleavage-defective mutants was due to the over-stabilization of hemophilic intercellular binding and to the absence of signal transduction by CTF2 from the cell surface N-cadherin. We therefore concluded that the cleavage of N-cadherin is essential for chondrocyte differentiation.

References

[1] S. Provot, E. Schipani, Molecular mechanisms of endochondral bone development, Biochem. Biophys. Res. Commun. 328 (2005) 658–665.
[2] M.B. Goldring, K. Tsuchimochi, K. Ijiri, The control of chondrogenesis, J. Cell Biochem. 97 (2006) 33–44.
[3] R.S. Tuan, Cellular signaling in developmental chondrogenesis: N-cadherin, Wnts, and BMP-2, J Bone Joint Surg. Am. 85-A (Suppl. 2) (2003) 137–141.
[4] R.S. Tuan, Biology of developmental and regenerative skeletogenesis, Clin. Orthop. Relat. Res. (2004) S105–S117.
[5] A. Woods, G. Wang, F. Beier, Regulation of chondrocyte differentiation by the actin cytoskeleton and adhesive interactions, J Cell Physiol. 213 (2007) 1–8.
[6] A.M. DeLise, R.S. Tuan, Alterations in the spatiotemporal expression pattern and function of N-cadherin inhibit cellular condensation and chondrogenesis of limb mesenchymal cells in vitro, J. Cell Biochem. 87 (2002) 342–359.
[7] S. Pokutta, K. Herrenknecht, R. Kemler, J. Engel, Conformational changes of the recombinant extracellular domain of E-cadherin upon calcium binding, Eur. J. Biochem. 223 (1994) 1019–1026.
[8] K.I. Tong, P. Yau, M. Overduin, S. Bagby, T. Porumb, M. Takeichi, M. Ikura, Purification and spectroscopic characterization of a recombinant amino-terminal polypeptide fragment of mouse epithelial cadherin, FEBS Lett. 352 (1994) 318–322.
[9] L. Shapiro, A.M. Fannon, P.D. Kwong, A. Thompson, M.S. Lehmann, G. Grubel, J.F. Legrand, J. Als-Nielsen, D.R. Colman, W.A. Hendrickson, Structural basis of cell–cell adhesion by cadherins, Nature 374 (1995) 327–337.
[10] H. Aberle, H. Schwartz, R. Kemler, Cadherin–catenin complex: protein interactions and their implications for cadherin function, J. Cell Biochem. 61 (1996) 514–523.
[11] T. Yagi, M. Takeichi, Cadherin superfamily genes: functions, genomic organization, and neurologic diversity, Genes Dev. 14 (2000) 1169–1180.
[12] R. Kemler, From cadherins to catenins: cytoplasmic protein interactions and regulation of cell adhesion, Trends Genet. 9 (1993) 317–321.
[13] T.S. Jou, D.B. Stewart, J. Stappert, W.J. Nelson, J.A. Marrs, Genetic and biochemical dissection of protein linkages in the cadherin–catenin complex, Proc. Natl. Acad. Sci. USA 92 (1995) 5067–5071.
[14] K. Uemura, T. Kihara, A. Kuzuya, K. Okawa, T. Nishimoto, H. Ninomiya, H. Sugimoto, A. Kinoshita, S. Shimohama, Characterization of sequential N-cadherin cleavage by ADAM10 and PS1, Neurosci. Lett. 402 (2006) 278–283.
[15] K. Reiss, T. Maretzky, A. Ludwig, T. Tousseyn, B. de Strooper, D. Hartmann, P. Saftig, ADAM10 cleavage of N-cadherin and regulation of cell-cell adhesion and beta-catenin nuclear signalling, Embo J. 24 (2005) 742–752.
[16] K. Reiss, P. Saftig, The "a disintegrin and metalloprotease" (ADAM) family of sheddases: physiological and cellular functions, Semin. Cell Dev. Biol. 20 (2009) 126–137.
[17] I.G. Haas, M. Frank, N. Veron, R. Kemler, Presenilin-dependent processing and nuclear function of gamma-protocadherins, J. Biol. Chem. 280 (2005) 9313–9319.
[18] T. Wakabayashi, A. Matsumine, S. Nakazora, M. Hasegawa, T. Iino, H. Ota, H. Sonoda, A. Sudo, A. Uchida, **Fbulin-3 negatively regulates chondro**, Biochem. Biophys. Res. Commun. 391 (2010) 1116–1121.
[19] K. Hatta, M. Takeichi, Expression of N-cadherin adhesion molecules associated with early morphogenetic events in chick development, Nature 320 (1986) 447–449.
[20] K. Hatta, S. Takagi, H. Fujisawa, M. Takeichi, Spatial and temporal expression pattern of N-cadherin cell adhesion molecules correlated with morphogenetic processes of chicken embryos, Dev. Biol. 120 (1987) 215–227.
[21] T. Fujimori, M. Takeichi, Disruption of epithelial cell–cell adhesion by exogenous expression of a mutated nonfunctional N-cadherin, Mol. Biol. Cell 4 (1993) 37–47.
[22] T. Fujimori, S. Miyatani, M. Takeichi, Ectopic expression of N-cadherin perturbs histogenesis in Xenopus embryos, Development 110 (1990) 97–104.
[23] A.R. Haas, R.S. Tuan, Chondrogenic differentiation of murine C3H10T1/2 multipotential mesenchymal cells: II. Stimulation by bone morphogenetic protein-2 requires modulation of N-cadherin expression and function, Differentiation 64 (1999) 77–89.
[24] S.A. Oberlender, R.S. Tuan, Expression and functional involvement of N-cadherin in embryonic limb chondrogenesis, Development 120 (1994) 177–187.
[25] S. Chubinskaya, G. Cs-Szabo, K.E. Kuettner, ADAM-10 message is expressed in human articular cartilage, J. Histochem. Cytochem. 46 (1998) 723–729.
[26] D.J. Dallas, P.G. Genever, A.J. Patton, M.I. Millichip, N. McKie, T.M. Skerry, Localization of ADAM10 and Notch receptors in bone, Bone 25 (1999) 9–15.
[27] E.J. Jin, K.S. Park, D. Kim, Y.S. Lee, J.K. Sonn, J.C. Jung, O.S. Bang, S.S. Kang, TGF-beta3 inhibits chondrogenesis by suppressing precartilage condensation through stimulation of N-cadherin shedding and reduction of cRREB-1 expression, Mol. Cells 29 (2010) 425–432.
[28] T.L. Le, A.S. Yap, J.L. Stow, Recycling of E-cadherin: a potential mechanism for regulating cadherin dynamics, J. Cell Biol. 146 (1999) 219–232.

THE JOURNAL OF BONE & JOINT SURGERY (BR)

■ ASPECTS OF CURRENT MANAGEMENT

Photodynamic therapy with acridine orange in musculoskeletal sarcomas

T. Matsubara,
K. Kusuzaki,
A. Matsumine,
H. Murata,
Y. Marunaka,
S. Hosogi,
A. Uchida,
A. Sudo

From Department of Cell Molecular Physiology, Kyoto Prefectural University Graduate School of Medical Science, Kyoto, Japan

■ T. Matsubara, MD, Orthopaedic Surgeon
■ A. Matsumine, MD, Assistant Professor
■ A. Uchida, MD, Dean
■ A. Sudo, MD, Professor
Department of Orthopaedic Surgery
Mie University Graduate School of Medicine, Edobashi 2-174 Tsu City, Mie 514-8507, Japan.

■ K. Kusuzaki, MD, Professor
■ Y. Marunaka, MD, Professor
■ S. Hosogi, MD, Research Fellow
Department of Molecular Cell Physiology
■ H. Murata, MD, Assistant Professor
Department of Orthopaedic Surgery
Kyota Prefectural University Graduate School of Medical Science, Kajii-cho 465 Kawaramachi-Hirokoji, Kamigyo-ku Kyoto 602-8566, Japan.

Correspondence should be sent to Professor K. Kusuzaki; e-mail: kusuzaki@koto.kpu-m.ac.jp

doi:10.1302/0301-620X.92B6.23788 $2.00

J Bone Joint Surg [Br] 2010;92-B:760-2.

Limb salvage involving wide resection and reconstruction is now well established for managing musculoskeletal sarcomas. However, involvement of major nerves and vessels with a large volume of muscle and skin may result in a useless limb, contributing to depression and a low quality of life. We have been studying alternative treatments for musculoskeletal sarcoma since 1990, and have recently established a regime using photodynamic surgery with cells labelled with acridine orange, photodynamic therapy with cells treated similarly and radiodynamic treatment using the effect of X-rays on such cells.

These techniques have been used after marginal or intra-lesional resection of tumours since 1999 and have enabled maintenance of excellent limb function in patients with sarcomas.

The use of photodynamic therapy (PDT) with haematoporphyrin or precursors such as porphyrin or aminoleuvelic acid has been shown to prevent local recurrence, when employed with minimally invasive surgery in early-stage superficial tumours of the skin, lung, oesophagus and bladder. The principle of this treatment is that a photosensitiser, such as haematoporphyrin, should first specifically or selectively accumulate in the tumour cells. Photon energy (hv) from a light source then excites the photosensitiser which activates intracytoplasmic oxygen. The activated oxygen oxidises fatty acids on the organelle (lysosomes membrane or DNA and RNA in the cell, resulting in death of the tumour cells due to necrosis or apoptosis. The targets of the photosensitisers differ. For example, haematoporphyrin groups bind to mitochondria.

As light beams, even from a laser system, cannot reach deeper than the skin or mucosa, sarcomas localised in deep areas are not suitable for PDT. However, irradiation of the tumour with a light beam is easily performed during surgery for resection of the tumour. If an incomplete intralesional procedure is performed accidentally, PDT might be useful in killing tumour cells which have leaked into the surgical area. We considered that if PDT could kill tumour cells, they might be eliminated without damage to normal tissues, preserving limb function without local recurrence.

Limb salvage with wide resection of the tumour followed by reconstruction using various types of endoprostheses, bone allograft or autograft in the treatment of musculoskeletal sarcomas has advanced markedly over the last 30 years.[1-5] However, satisfactory recovery of function may not be achieved and most patients are still not able to run or swim fast, jump confidently, or throw a ball a long distance.[6-8] These disabilities limit the activity of the patients. Better means of achieving satisfactory recovery of function after limb salvage are needed. We have therefore been investigating new photodynamic therapies since 1990.[9-13] The use of haematoporphyrin may result in dermatitis induced by light and it requires a relatively long time to accumulate in tumour tissue. PDT with haematoporphyrin also requires the use of expensive laser beams. We therefore employed acridine orange (AO) as a photosensitiser. This was extracted from coal tar in the late 19th century as a weak basic dye for staining clothes or microorganisms. Its biological properties include antitumour activity,[14,15] photosensitising activity,[16,17] and toxicity against bacteria, malarial parasites, and fungi.[17-21] It has a low molecular weight of 463u, and is reported to be capable of rapid flow into the cytoplasm through the cell membrane to bind to DNA,[22] RNA[23] and lysosomes.[24] Many experimental studies have shown that AO has properties as a photosensitiser and is useful for PDT in the treatment of cancer.[25-29] However, the clinical application of AO in cancer therapy has not been described. This may be because of the potential

toxic effects of AO, which has been reported to induce mutagenic activity in bacteria.[18,19] The carcinogenicity of AO has yet to be confirmed experimentally.[30] An International Agency for Research on Cancer (IARC) report[31] in 1978 classified AO into group 3, meaning that the agent is not currently classifiable in terms of carcinogenicity in humans. The local administration of AO to patients for screening for gastric and cervical cancer has been described,[32] but none have developed new cancers induced by AO during the current follow-up of 11 years.

Our basic studies have shown that AO binds densely to lysosomes and acidic vesicles, emitting orange fluorescence after excitation by blue light in viable cultured mouse osteosarcoma cells and binds sparsely to RNA, emitting green fluorescence after excitation. AO has a unique feature in that the polymer type emits orange fluorescence, whereas the monomer shows green fluorescence under excitation by blue light.[13] Osteosarcoma cells transplanted into mice emitted green fluorescence after intraperitoneal or intravenous injection of AO followed by blue light excitation, while normal muscle and adipose tissue cells did not. Hence, tumours could be visually localised under a fluorescence surgical microscope, through an effect of fluorovisualisation.[12] We have confirmed that most human malignant bone and soft-tissue tumours are sensitive to staining with AO, as specimens which have been resected emit intense green fluorescence after exposure to a solution of AO with blue light excitation. Although the mechanisms underlying selective binding of AO to musculoskeletal sarcoma are unclear, staining with AO is useful for visualising the tumour during surgery under fluorescence microscopy. We also found that AO had a strong cytocidal effect on mouse osteosarcoma cells after blue light excitation, both *in vitro*[9] and *in vivo*,[10] suggesting that it might be useful for PDT against musculoskeletal sarcoma. Since the concentration of AO solution (1 μg/ml) used in our clinical study was very low, and it was only administered locally, we believe that the risk of carcinogenesis induced by AO in patients may be significantly lower than that occurring from most other known anticancer agents.

When using porphyrin or its derivatives for PDT,[33] a laser beam with high energy focused over a narrow area is commonly used as the excitation light source. With AO we have used a high-power xenon lamp (SANEI Electric MIG Co., Ltd., Tokyo, Japan), since blue light illumination over a wide area is necessary for fluorovisualisation of AO and for the strong cytocidal effect of AO-PDT on the tumour cells spread widely throughout the surgical field during curettage. Xenon lamps are much cheaper than lasers. A recent study has shown that the cytocidal effect of AO-PDT is dependent not only on the wavelength (blue light, 466.5 nm), but also on the lux (lx) value of the light. Hence, while blue light needs to be used for microscopic curettage, full-wave light obtained from the xenon lamp without an interference filter is more effective than blue light alone for AO-PDT, because of the much higher lux of the lamp. We have therefore slightly modified our technique of AO-PDT during the last two years by using full-wave light.

Before the application of AO-PDT to human sarcomas, we carried out a simulation study of curettage supported by AO-PDT, using a mouse model.[10] This showed that AO-PDT after macroscopic and microscopic curettage of a mouse osteosarcoma significantly inhibited local recurrence of the tumour. The rate of recurrence in the control group was 80%, compared with only 23% in the group-treated using AO-PDT. We also observed that low-dose X-ray irradiation of 5 Gy to mouse osteosarcoma after exposure to AO (radiodynamic therapy with acridine orange: AO-RDT) showed the same strong cytocidal effect as that of AO-PDT.[11] Such irradiation has the advantage of reaching deeper areas of the human body compared with a light beam, although the deleterious effects on normal tissues are greater. The results of these basic studies suggest that AO-PDT and AO-RDT might be applicable for limb salvage in patients with malignant tumours of bone and soft tissue. If effective, patients might recover almost full limb function, with only a low risk of local recurrence.

We therefore conducted a clinical study to determine the feasibility and usefulness of AO-PDT with AO-RDT in human musculoskeletal sarcomas. We found an overall rate of recurrence of 10%, almost the same as that after wide resection of the tumour.[34-36] None of the five patients who had received AO-PDT with AO-RDT had recurrent tumour during a follow-up of more than two years. In the one case treated with AO-PDT alone the tumour recurred after 21 months, longer than would have been expected after macroscopic curettage of high-grade malignant sarcoma. Although the duration of follow-up was relatively short, we are convinced that the treatment employed was beneficial. The use of AO-PDT with, or without AO-RDT, inhibits local recurrence of musculoskeletal sarcomas, as most high-grade malignant sarcomas will recur within six months after intralesional excision.[34-36] However, it is uncertain for how long this treatment might remain effective.

With the exception of one patient, the function of the limb was restored to the pre-operative level, and all patients were satisfied with the recovery of function. Compared with the results after wide resection of the tumour followed by limb reconstruction, recovery of function after AO-PDT (with or without AO-RDT) was superior in our study. We expect these patients to spend the remainder of their lives as normal, non-handicapped individuals. Local administration of AO, AO-PDT or AO-RDT was not associated with any complications, such as skin hypersensitivity to light, which is often encountered with PDT using porphyrin or its derivatives,[33] and the patient does not need to avoid exposure to the sun even in the early phase after surgery.

AO-PDT with or without AO-RDT appears to be a promising new regime for the preservation of limb function in patients with a musculoskeletal sarcoma. This approach may also be applicable to other solid tumours, although larger studies with follow-up are required.